MITLibraries | DSpace@MIT

MIT Open Access Articles

Rationalizing the Spatial Distribution of Mesoscale Eddy Diffusivity in Terms of Mixing Length Theory

Massachusetts Institute of Technology

Rationalizing the Spatial Distribution of Mesoscale Eddy Diffusivity in Terms of Mixing Length Theory

MICHAEL BATES,* ROSS TULLOCH, JOHN MARSHALL, AND RAFFAELE FERRARI

Department of Earth, Atmospheric and Planetary Sciences, Massachusetts Institute of Technology, Cambridge, Massachusetts

ABSTRACT

Observations and theory suggest that lateral mixing by mesoscale ocean eddies only reaches its maximum potential at steering levels, surfaces at which the propagation speed of eddies approaches that of the mean flow. Away from steering levels, mixing is strongly suppressed because the mixing length is smaller than the eddy scale, thus reducing the mixing rates. The suppression is particularly pronounced in strong currents where mesoscale eddies are most energetic. Here, a framework for parameterizing eddy mixing is explored that attempts to capture this suppression. An expression of the surface eddy diffusivity proposed by Ferrari and Nikurashin is evaluated using observations of eddy kinetic energy, eddy scale, and eddy propagation speed. The resulting global maps of eddy diffusivity have a broad correspondence with recent estimates of diffusivity based on the rate at which tracer contours are stretched by altimetric-derived surface currents. Finally, the expression for the eddy diffusivity is extrapolated in the vertical to infer the eddy-induced meridional heat transport and the overturning streamfunction.

1. Introduction

The oceans are replete with mesoscale eddies and associated turbulence. These time-dependent motions are an integral part of the general circulation, playing a significant role in the mixing and stirring of tracers. The rate at which mesoscale eddies mix can be characterized in terms of an eddy diffusivity that has a value on the order of $1000 \, \mathrm{m^2 \, s^{-1}}$. However, it is clear that this canonical value is only a reference: in reality the ocean's mesoscale eddy diffusivity is far from constant in space or time but instead exhibits considerable variability (e.g., Davis 1991; Holloway 1986; Ledwell et al. 1998; Marshall et al. 2006; Abernathey et al. 2010; Naveira Garabato et al. 2011).

Eddy transfer is thought to be of leading order importance in dynamical balances in the ocean and the distribution of tracers therein, particularly in the Southern Ocean (see Marshall and Speer 2012). Therefore, coarse-resolution models that do not resolve mesoscale eddies must parameterize their effect. This is typically achieved by mixing tracers along neutral surfaces, as suggested by Redi (1982), and by modifying the advective process by introducing an eddy-induced flow pioneered by Gent and McWilliams (1990). Such schemes often use a spatially and temporally constant diffusivity [see, e.g., the models described in Griffies et al. (2009)]. However, as shown by, for example, Ferreira et al. (2005) and Danabasoglu and Marshall (2007), if one allows eddy diffusivities to vary in space, systemic drifts in climate models can be reduced. Moreover, the response of models to changes in external forcing (such as trends in Southern Ocean winds due to anthropogenic forcing) is found to depend on the form of the eddy closure employed. A further complication arises because the along-isopycnal diffusivity for tracers (Redi 1982) and the diffusivity used to close for the eddy-induced circulation may not be the same, a point emphasized by Smith and Marshall (2009). Here, we focus on an eddy diffusivity that can be used for tracers—including potential vorticity—that depends on the state of the large-scale flow and so can change as the climate changes.

* Current affiliation: Griffith School of Environment, Griffith University, Brisbane, Queensland, Australia.

Corresponding author address: Michael Bates, Griffith School of Environment, Griffith University, 170 Kessels Rd., Nathan, QLD 4111, Australia.
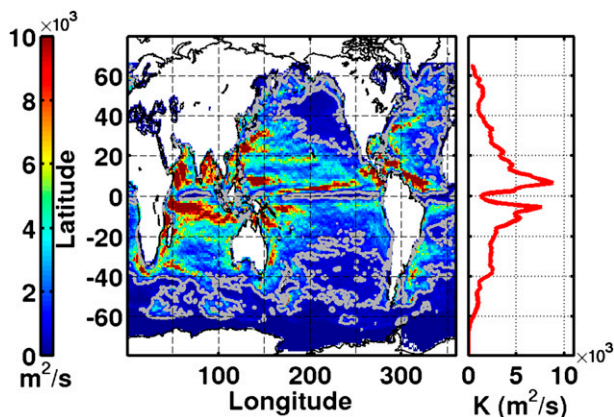E-mail: m.bates@griffith.edu.au

FIG. 1. The effective diffusivity ($m^2 s^{-1}$) at the ocean's surface from Abernathey and Marshall (2013). The gray contours are isolines of $1000 \, m^2 \, s^{-1}$. (left) A map where the color is saturated at $K_{eff} = 10\,000 \, m^2 \, s^{-1}$. (right) The zonally averaged effective diffusivity.

Recently, Abernathey and Marshall (2013) estimated the surface cross-stream eddy diffusivity for passive tracers by diagnosing the part of the downgradient eddy flux associated with irreversible mixing using the Osborn and Cox (1972) relation, as described in section 2. They show overall agreement with the effective diffusivity of Nakamura (1996) that also quantifies the enhancement of mixing due to finescale features created by eddy stirring. Importantly, the diffusivity from the Osborn and Cox (1972) relation and the effective diffusivity both characterize mixing across mean tracer gradients. The spatial map of the effective diffusivity K_{eff} from Abernathey and Marshall (2013) is shown in Fig. 1. It is clear that there is a high degree of heterogeneity with values considerably larger and considerably smaller than the canonical $1000 \, m^2 \, s^{-1}$.

The most direct measurement of the surface diffusivity is from satellite-tracked drifters. The single-particle diffusivity based on drifters is equivalent to that estimated from tracer fluxes if the number of drifters is sufficiently large (Klocker et al. 2012a,b). Zhurbas and Oh (2004) produced a global map of surface diffusivity based on drifter data. Their map does not reveal the suppression of mixing in the core of mean currents reported by Abernathey and Marshall (2013). Klocker et al. (2012b) show that it is extremely difficult to capture the suppression of the diffusivity from Lagrangian data because the suppression is associated with a negative lobe in the velocity autocorrelation function at long lags on the order of a month [see also Swenson and Niiler (1996)]. Hundreds of drifters are required to accurately estimate the velocity autocorrelation function at such long lags, but no more than tens of drifters are ever available in any patch of ocean. Poulain and Niiler (1989) and many authors since have resorted to estimating an upper bound on the diffusivity by ignoring the negative lobe. This

is tantamount to ignoring the suppression. We believe that these problems are manifest in the extreme large values of surface diffusivity in the map of Zhurbas and Oh (2004), which often exceed $10\,000 \, m^2 \, s^{-1}$. Using drifters, Sallée et al. (2008) proposed to fit an analytical expression to the observed autocorrelation function, which includes a negative lobe. Sallée et al. (2011) also used drifter data to estimate a diffusivity in the Southern Ocean by averaging over days 250–360 to avoid missing the lobes and thereby capturing the effects of suppression. While these approaches are more in line with our work, the statistical uncertainty at long lags remains an issue in the estimation of suppression. While the use of tracer-derived diffusivities have their own associated uncertainty and drawbacks, given that our paper focuses on suppression of mixing over the entire globe, we prefer to compare our results against the surface diffusivity map of Abernathey and Marshall (2013, shown in Fig. 1).

Our goal is to rationalize the surface spatial patterns of K_{eff} shown in Fig. 1 using classical mixing length theory (Taylor 1922; Prandtl 1925). This eddy diffusivity (which is equivalent to a single-particle diffusivity; see Klocker et al. 2012a) is expressed as the product of the root-mean-square (rms) eddy velocity u_{rms} and the scale over which parcels of fluid are transferred by the eddies and then mixed, as measured by the mixing length L_{mix} as follows:

$$K = u_{rms} L_{mix}. \tag{1}$$

The mixing length is the characteristic distance that a fluid parcel travels before being mixed and is analogous to the mean free path in thermodynamics. Sometimes, Eq. (1) is written with a "mixing efficiency"; here we absorb the mixing efficiency into the definition of the mixing length.

Mixing length theory has been the basis for several attempts to estimate the eddy diffusivity in the ocean both from data and models including, for example, the studies of Visbeck et al. (1997), Eden and Greatbatch (2008), and Ferrari and Nikurashin (2010). Here, we use observationally based estimates of u_{rms} and L_{mix} to yield an eddy diffusivity based on Eq. (1) that is then compared to that diagnosed by Abernathey and Marshall (2013). We find that steering level effects play a very significant role in modulating the mixing length (see Bretherton 1966; Green 1970; Stone 1972; Killworth 1997; Smith and Marshall 2009; Ferrari and Nikurashin 2010; Klocker and Abernathey 2014) and contribute to rich spatial structure in the eddy diffusivity.

Our manuscript is set out as follows. In section 2, the horizontal distribution of K at the ocean's surface is interpreted in terms of mixing length theory. In particular, we examine the importance of the suppression of

mixing due to the steering level effects and discuss the limitations and uncertainty in the associated theory. Section 3 then applies the insights developed for the surface problem to the subsurface, obtaining estimates of the interior distribution of diffusivity. Section 4 uses the resulting three-dimensional distributions of eddy diffusivity to estimate the eddy-induced overturning circulation in the Southern Ocean and compares it to one calculated using a constant diffusivity. Finally, we conclude in section 5.

2. The surface eddy diffusivity

Here, maps of surface eddy diffusivity are computed using Eq. (1) with u_{rms} estimated from altimetry and L_{mix} estimated from the theory and data reviewed below. These are then compared to the map produced by Abernathey and Marshall (2013), which is shown in Fig. 1.

Abernathey and Marshall (2013) estimated a diffusivity by advecting numerical tracers with the geostrophic velocity obtained from altimetry. The velocity field deformed the initially smooth tracer profiles into a tangle of contorted filaments. The eddy diffusivity was computed from the twisted tracer distributions using the Osborn and Cox (1972) relation,

$$K_{OC}(x,y) \equiv \frac{\chi}{|\nabla \overline{T}|^2}, \qquad (2)$$

where χ is the dissipation of tracer variance and $|\nabla \overline{T}|^2$ is the gradient of the coarse grain–averaged tracer concentration.

Two tracers were used: one was initially aligned along latitude circles and the other was aligned with the streamfunction for the mean horizontal flow. The minimum of the diffusivity based on each tracer was used, and the map is interpreted as a cross-stream/zonal eddy diffusivity. Because Eq. (2) assumes that the tracer variance is locally generated and dissipated, it is thus meaningful only when averaged over large ocean patches. When using the map of Abernathey and Marshall (2013) to ground our results based on Eq. (1), we will therefore focus on broad-scale patterns rather than small-scale variations.

a. Estimates of eddy velocity, eddy scales, and implied mixing rates

The rms eddy velocity is defined as $u_{rms}^2 = (1/2)(\overline{u'^2} + \overline{v'^2})$, where u' and v' are the fluctuating eddy velocities. The altimeter product used for u_{rms} estimates the rms geostrophic eddy velocity from sea surface height anomalies and was produced by Segment Sol multimissions d'ALTimétrie, d'Orbitographie et de localisation précise/Data Unification and Altimeter

Combination System (SSALTO/DUACS) and distributed by the Archiving, Validation, and Interpretation of Satellite Oceanographic data (AVISO), with support from the Centre National d'Études Spatiales (CNES) (http://www.aviso.oceanobs.com/duacs/). We use the AVISO dataset to be consistent with our baseline diffusivity from Abernathey and Marshall (2013). Surface velocities are computed by taking finite differences of sea surface height and assuming geostrophic balance, except within 5° of latitude of the equator, where a β-plane formulation of geostrophic balance is used following Lagerloef et al. (1999). The global map of u_{rms}^2 is shown in Fig. 2a. Western boundary currents (WBCs), like the Gulf Stream, Kuroshio, East Australia Current, Agulhas Current, and Antarctic Circumpolar Current (ACC), are prominent kinetic energy maxima. The discontinuities across $\pm 5°$ of latitude reflect the transition from the f-plane to the β-plane formulation of geostrophic balance.

The mixing length is conceptually analogous to the mean free path in thermodynamics; a fluid parcel will conserve its properties for a characteristic length, before mixing with the surrounding fluid. In the oceanographic literature, it is often assumed that the mixing length scales with the size of the energy-containing eddies (e.g., Holloway 1986; Haine and Marshall 1998). However, the mixing length can be much larger than the eddy scale, if eddies are so strongly nonlinear as to trap fluid and travel erratically long distances before mixing it with the surrounding fluid (e.g., Thompson and Young 2006). The mixing length can also be smaller than the eddy size, if eddies are very weakly nonlinear and hardly displace fluid parcels. Altimetric observations show that oceanic eddies are nonlinear (Chelton et al. 2011), but not so strongly as to propagate in an erratic fashion. Recent work by Klocker and Abernathey (2014) provides evidence that, in the absence of mean flows, the mixing length does indeed scale directly with the eddy diameter.

Observations indicate that oceanic eddies typically propagate along and not across potential vorticity contours (Marshall et al. 2006). The oceanic potential vorticity contours are zonal in much of the ocean (particularly the Southern Ocean) and follow the mean currents where there are strong flows. Hence, eddy propagation in the ocean does not act to increase meridional/across mean–current mixing. Rather, Ferrari and Nikurashin (2010) find that the across potential vorticity gradient mixing length is proportional to the eddy scale, but it is suppressed if eddies propagate at different speeds from the mean flow.

To gain insight in what parameters dominate variations in the eddy diffusivity, Fig. 3 compares the meridional structure of the zonally averaged K_{eff} of Abernathey and
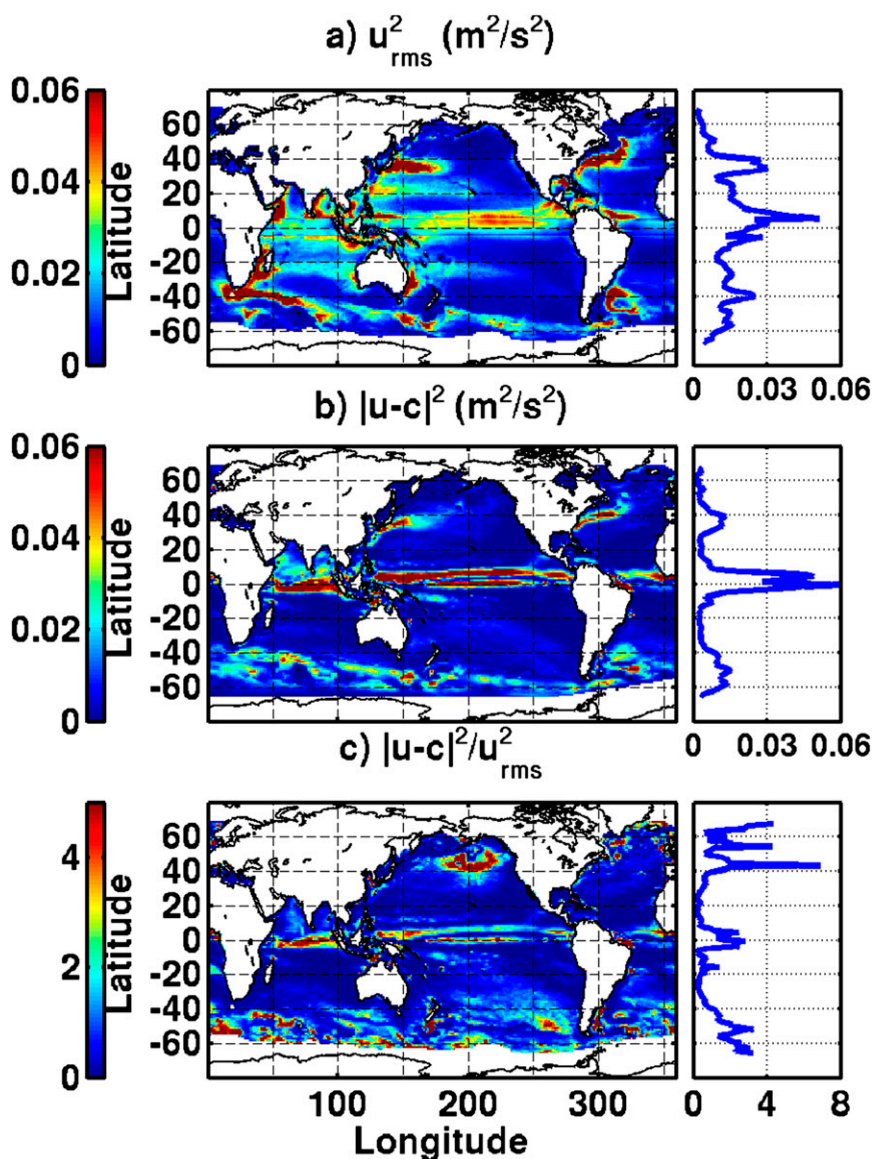
FIG. 2. (a) The square of the rms eddy speed u_{rms}^2, (b) the square of the difference between the mean velocity and eddy phase speed $|\bar{u} - c|^2$, and (c) the ratio $|\bar{u} - c|^2/u_{rms}^2$, which gives an indication of the strength of suppression [see Eq. (6)].

Marshall (2013), the zonally averaged eddy diameter map of Chelton et al. (2011), and the zonally averaged u_{rms} from AVISO. The overall decrease of K_{eff} toward the poles appears to track the decrease in eddy diameter, rather than the less pronounced, irregular variations in rms eddy velocity. Of interest is the sudden decrease of K_{eff} at the equator despite the fact that both the eddy size and rms eddy velocity are largest there. It will be shown below that these variations are consistent the idea that in the deep tropics eddies propagate at speeds that are much larger than mean currents, thus suppressing mixing.

As a first step, we calculate the eddy diffusivity using Eq. (1) by setting the mixing length to the eddy diameter multiplied by 0.35 [the factor of 0.35 was empirically determined by Klocker and Abernathey (2014) and is held at this constant value here; see appendix A] and using AVISO to estimate u_{rms}. The resulting map of the surface diffusivity is shown in Fig. 4 and should be compared with Fig. 1. It is clear that the eddy diffusivity is overestimated almost everywhere. Moreover, this cannot be "fixed" by simply scaling down the mixing length because the degree of overestimation varies with latitude and is particularly noticeable in the
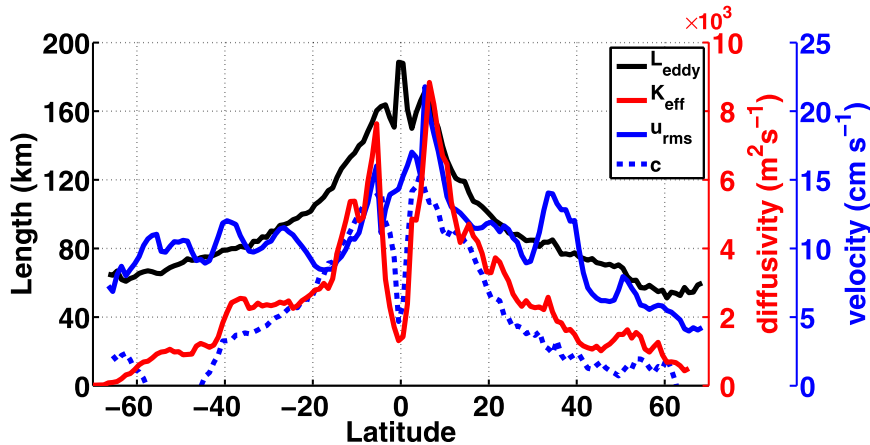
FIG. 3. The zonally averaged diffusivity K_{eff} of Abernathey and Marshall (2013, red), the zonally averaged eddy diameter L_{eddy} (solid black) of Chelton et al. (2011), the AVISO rms velocity u_{rms} (solid blue), and the Hughes westward zonal eddy phase speed c (i.e., westward is positive; dashed blue). The color of the curves corresponds to the color of the vertical axis (black corresponds to length, red corresponds to diffusivity, and blue corresponds to velocity).

tropics. In the next section, we review the theory that quantifies the reduction in mixing due to steering level effects.

b. The role of eddy propagation in modulating mixing

Mixing by geostrophic eddies and turbulence can be strongly modulated by interactions with the mean flow. This notion is well established in the atmospheric literature and was pioneered by Bretherton (1966), Green (1970), and Stone (1972). There is a growing, parallel literature in the ocean context (e.g., Bower 1991; Lozier and Bercovici 1992; Bower and Lozier 1994; Smith and Marshall 2009; Abernathey et al. 2010; Ferrari and Nikurashin 2010). Ferrari and Nikurashin (2010) showed that in the Southern Ocean if the mixing length is set equal to the eddy scale, as in Holloway (1986), the resulting diffusivities are inconsistent with diagnostic estimates of the eddy diffusivity found. Most of the oceanographic literature on the suppression of mixing by steering level effects is focused on the ACC, where these effects are significant, and the geometry is simple and somewhat similar to the atmosphere. However, such effects are also likely to be significant in other regions where eddies and jets coexist, such as western boundary currents and equatorial regions. We now briefly review key elements of "mixing theory" in which waves moving zonally with phase speed c along a mean zonal flow $\overline{u}$ induce fluid parcels to move transverse to the mean flow, thus transferring properties in the cross-stream direction. We then go on to assess whether these effects can account for some of the differences between Figs. 1 and 4.

1) LINEAR MIXING THEORY

By considering the growth of a linearly unstable baroclinic wave, Bretherton (1966) and Green (1970) derived an eddy diffusivity that depends on eddy kinetic energy, the mean current, the growth rate, and propagation phase speed of the most unstable waves. As a perturbative linear model, it is only able to predict the spatial variation of mixing and not the amplitude. Nevertheless, it emphasizes the tendency of eddy propagation to suppress mixing and the importance of steering
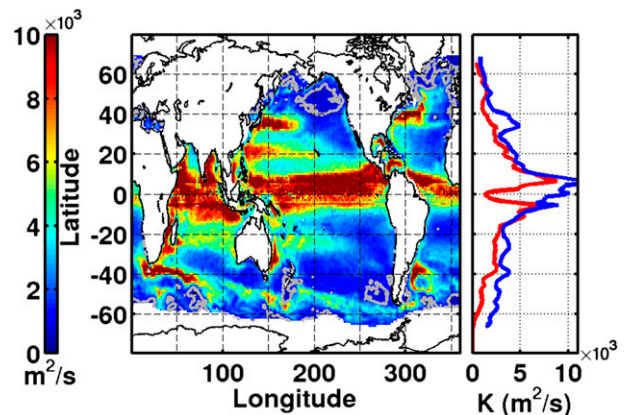
FIG. 4. The predicted eddy diffusivity ($m^2 s^{-1}$) from the unmodulated mixing length theory, where the mixing length is set to the eddy diameter multiplied by 0.35 in Eq. (1). Here the eddy velocity u_{rms} is derived from AVISO altimetry data; the eddy diameter L_{eddy} is taken from Chelton et al. (2011). (left) A map where the gray line is an isoline of $1000 \, m^2 s^{-1}$. (right) The zonal average of the left panel (blue) and the zonally averaged diffusivity of Abernathey and Marshall (2013; see also Fig. 1, red).

levels at which the eddy propagation speed matches the mean flow speed.

When a linear wave of the form

$$v' = \text{Re}\{F(y, z) \exp[i(kx + \ell y - \omega t)]\} \qquad (3)$$

is assumed for the meridional velocity, diffusion of quasigeostrophic potential vorticity has the form

$$K^{\text{Green}} = \frac{\omega_i |u'|^2}{2k^2(\omega_i^2/k^2 + |\bar{u} - c|^2)}, \qquad (4)$$

where x is the zonal coordinate, y is the meridional coordinate, z is the vertical coordinate, t is time, F is a function that describes the meridional and vertical structure, ω_i is the baroclinic growth rate, c is the real part of the phase speed, and (k, ℓ) are the zonal and meridional wavenumbers (Bretherton 1966; Green 1970). Green (1970) hypothesizes that the growing kinetic energy of a linear wave $|u'|^2$ can be replaced by the turbulent eddy kinetic energy u_{rms}^2. If one further assumes that the turbulence is isotropic (which is reasonable outside of the tropics), the zonal wavenumber can be replaced by the isotropic wavenumber $|\mathbf{k}|^2 = 2k^2$. Equation (4) was the form used by Marshall (1981) in his study of the parameterization of eddy fluxes in a zonal two-level quasigeostrophic channel flow.

2) STOCHASTIC MIXING THEORY

Ocean eddies are nonlinear, and it is not clear how to interpret the quantities that appear in Eq. (3). In particular, eddies are not continuously growing at some rate ω_i, rather they rapidly grow and slowly decay, reaching a statistical equilibrium. Ferrari and Nikurashin (2010) showed that an equation similar to Eq. (4) can be derived by considering the mixing induced by a random superposition of Rossby waves growing very rapidly, decaying at some slower rate γ, and propagating at a speed c obtaining

$$K^{\text{FN}} = \frac{\gamma u_{\text{rms}}^2}{|\mathbf{k}|^2(\gamma^2/k^2 + |\bar{u} - c|^2)}. \qquad (5)$$

The damping rate γ, or more appropriately the inverse eddy decorrelation time scale, represents the eddy lifetime. If γ is proportional to the linear growth rate ω_i, then Eqs. (4) and (5) are identical. However, in nonlinear eddy fields, γ is typically proportional to the eddy turnover time and not to the growth rate (Salmon 1998).

Here we assume that the theory underlying Eq. (5) is equally valid in the subsurface as at the surface, the validity of which is somewhat ambiguous and is an issue we shall explore in more detail in section 3. Appendix A outlines in detail the assumptions we make in order to extrapolate the surface theory. In brief, these assumptions are that the inverse eddy decorrelation time scale is proportional to the eddy turnover rate $\gamma \propto |\mathbf{k}|u_{\text{rms}}$ at the surface, that the eddies are equivalent barotropic, that the energy-containing eddies are isotropic $|\mathbf{k}|^2 = 2k^2$, that the eddies propagate at a characteristic speed c, that the eddy phase velocity is predominantly zonal, and that the eddy diameter is related to the eddy wavenumber by $L_{\text{eddy}} = 2\pi/|\mathbf{k}|$; we then obtain

$$K = u_{\text{rms}} \frac{\Gamma L_{\text{eddy}}}{1 + b_1 |\bar{u} - c|^2/u_{\text{rms}}^2(z = 0)}, \qquad (6)$$

where Γ and b_1 are constants to be determined, and L_{eddy} is the eddy diameter. Equation (6) is the form we use for our calculations.

Klocker and Abernathey (2014) provide an estimate of the parameters Γ and b_1 (see also appendix A) in a region of the eastern Pacific and confirm that the unsuppressed diffusivity is proportional to the eddy size. They arrive at this conclusion by driving a model of the eastern Pacific with geostrophic eddy velocities inferred from AVISO altimetry and by varying the mean zonal velocity. The mean zonal velocity where the diffusivity is a maximum corresponds to an unsuppressed diffusivity (i.e., $\bar{u} = c$), allowing them to both confirm the relationship with the eddy length scale and also infer that $\Gamma = 0.35$. Appendix A outlines how we use their results [and that of Ferrari and Nikurashin (2010)] to deduce that $b_1 \approx 4$. We use these values throughout this manuscript, except in sections 2c and 3 where we examine the sensitivity of the diffusivity to the magnitude of b_1.

The diffusivity in Eq. (6) can be compared to the mixing length formula in Eq. (1) to infer that the eddy propagation modulates the mixing length scale as

$$L_{\text{mix}} = \frac{\Gamma L_{\text{eddy}}}{1 + b_1 |\bar{u} - c|^2/u_{\text{rms}}^2(z = 0)}. \qquad (7)$$

The denominator of Eq. (7) is always greater than or equal to one and represents the suppression of mixing by eddy propagation; when eddies propagate at a speed different from the mean flow, some of the tracer can be advected out of the eddy before it is fully mixed (Ferrari and Nikurashin 2010). The suppression factor is defined as

$$\frac{1}{1 + b_1 |\bar{u} - c|/u_{\text{rms}}^2(z = 0)}, \qquad (8)$$

which is always between zero and one. Suppression is absent at steering levels where $c = \bar{u}$, and the mixing length is directly proportional to the eddy diameter.
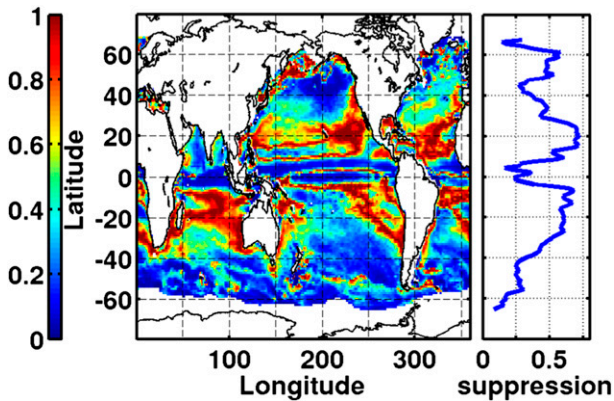
FIG. 5. The suppression factor $[1 + b_1|\overline{u} - c|^2/u_{\mathrm{rms}}^2]^{-1}$ [cf. Eq. (7); nondimensional] at the surface with $b_1 = 4$ as a (left) map and (right) zonal average. AVISO data are used for the eddy velocity u_{rms}, ECCO data are used for the surface mean velocity $\overline{u}$, and the phase speed is taken from the dataset of Hughes.

c. Refined predictions of the surface eddy diffusivity

The suppression factor is evaluated at the surface and shown in Fig. 5. The eddy phase speed was provided by Hughes who estimated it from altimetry (see Hughes et al. 1998; Hughes 2005; Tulloch et al. 2009), the zonal-mean velocity $\overline{u}$ is from the Estimating the Circulation & Climate of the Ocean (ECCO) state estimate (Wunsch et al. 2009), u_{rms} is the eddy rms velocity inferred from AVISO sea surface height anomalies, and we set $b_1 = 4$. A small difference in the zonal flow and eddy phase speed $|\overline{u} - c|$ (see Fig. 2b) can imply weak suppression, while a small u_{rms}^2 can enhance suppression (see Fig. 2a). The resulting patterns are a complex interplay between $|\overline{u} - c|^2$ and u_{rms}^2, setting their ratio (see Fig. 2c). There are vast areas, such as in the North and South Pacific, where there is strong suppression caused by a small u_{rms} and moderate values of $|\overline{u} - c|$. Conversely, there are regions of weak suppression, such as the Indian Ocean west of Australia, due to moderate u_{rms} and small values of $|\overline{u} - c|$. Throughout much of the equatorial ocean, there are alternating bands of strong and weak suppression. Our analysis agrees with that of Abernathey and Marshall (2013) that these bands are largely due to the presence of strong zonal currents of alternating direction, such as the North Equatorial Current, North Equatorial Countercurrent, and South Equatorial Current.

We wish to gain some insight into the skill of Eq. (6). Accordingly Fig. 6 compares estimated probability density functions of the effective diffusivity of Abernathey and Marshall (2013), K_{eff}, with that of our predicted diffusivity with no suppression ($b_1 = 0$) and an increasing amount of suppression ($b_1 = 1$ and 4). We plot the probability density functions for four regions: the

southern and northern high latitudes, midlatitudes, and the tropics, as indicated in the legend. Including the suppression factor eliminates the significant bias toward large diffusivities in all regions. However, the optimal value of b_1 appears to vary somewhat regionally with a suggestion that a smaller value ($b_1 = 1$) is more appropriate in the tropics, and a medium value ($b_1 = 4$) is more appropriate in the southern high latitudes. Given that we do not currently have a robust theory to estimate b_1 regionally, we choose to keep it globally constant and adopt $b_1 = 4$ as our optimum choice. This does a reasonably good job in all regions and particularly in the southern high latitudes where we know eddy processes, and thus parameterization of those processes, is the most critical.

In summary we draw the following broad conclusions:

(i) The inclusion of steering level effects reduces the systematic overestimation implied by the unsuppressed diffusivity. When compared to the map of Abernathey and Marshall (2013), including suppression eliminates the significant bias toward large values in all regions. Quantitative comparison suggests that $b_1 = 4$ gives an optimum level of suppression. This value is broadly consistent with prior estimates in Klocker and Abernathey (2014) and Ferrari and Nikurashin (2010).

(ii) Broad patterns in the diffusivity emerge that are a consequence of suppression and not merely associated with the spatial distributions of u_{rms}. Compare Figs. 1, 4, and 7.

(iii) Eddy diffusivities are strongly suppressed in the tropics (Fig. 5) because $|\overline{u} - c|^2/u_{\mathrm{rms}}^2 \gg 1$ there (Fig. 2c), reducing the unrealistically large values of mixing in the unsuppressed map (Fig. 4).

3. The subsurface eddy diffusivity

A full theory of mixing by geostrophic eddies requires that we extend the analysis of the surface eddy diffusivity to the whole ocean column. However, the scaling law in Eq. (6), which is the cornerstone of this paper, has not yet been validated against numerical simulations or observations. Here, we take the bold move of assuming that Eq. (6) holds at all depths in the ocean and we will compare its predictions against the observations of the vertical structure of the eddy diffusivity in the real ocean. Consistent with the interpretation of Eq. (6) given in the previous sections, we assume that the eddy size L_{eddy} and the phase speed c are depth independent, because they cannot vary with depth if the eddy is to propagate as a coherent structure over the water
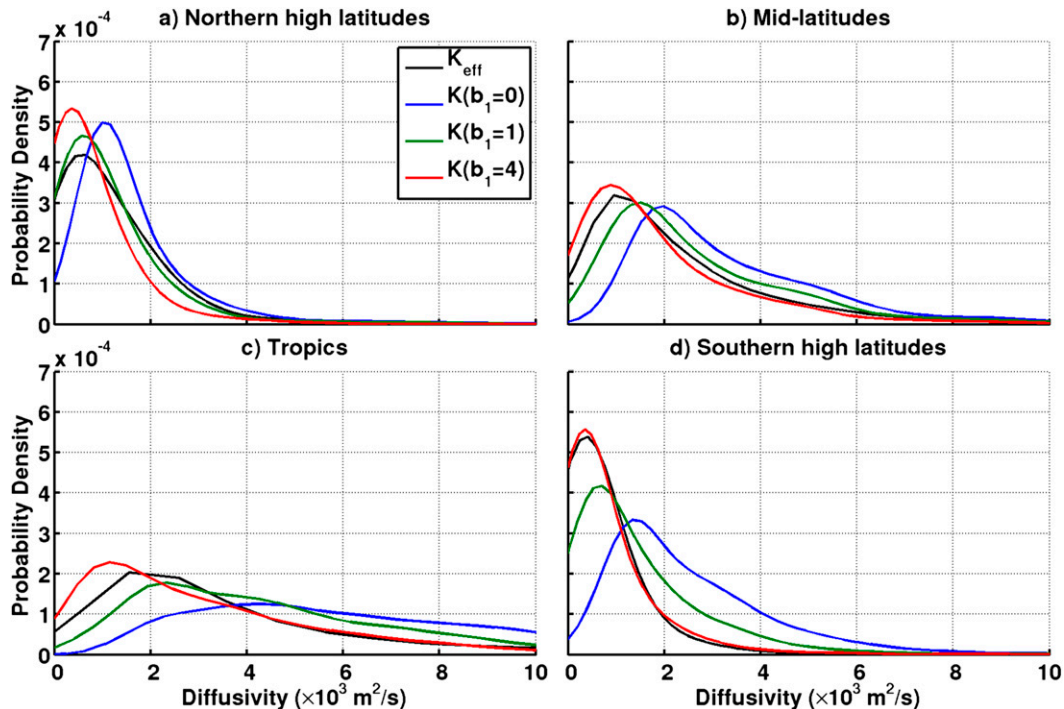
FIG. 6. The probability density function of diffusivity for (a) high northern latitudes (north of 40°N), (b) mid-latitudes (40°–20°S and 20°–40°N), (c) the tropics (20°S–20°N), and (d) southern high latitudes (south of 40°S). The diffusivity of Abernathey and Marshall (2013, black) and the diffusivity using Eq. (6) with $b_1 = 0$ (corresponds to no suppression; blue), $b_1 = 1$ (green), and $b_1 = 4$ (red) are shown.

column. The mean and u_{rms} velocities are instead taken to be depth dependent and will be computed from the ECCO (Wunsch et al. 2009) and ECCO phase II (ECCO2; Menemenlis et al. 2008) state estimates respectively, averaged onto our 1° grid.

a. Estimating the subsurface eddy diffusivity

As shown in section 2, suppression at the surface plays an important role in modulating the eddy diffusivity. But what might its effect be in the ocean interior? Figure 8 shows the zonally averaged suppression factor [Eq. (8)], which modulates the mixing length. At mid- and high latitudes there is significant suppression at the surface implying a mixing length that is typically only half the eddy scale. Suppression at depth is less strong, except in the tropics. Indeed, in the tropics there is strong suppression at all depths. The broad geography of suppression in the extratropics is consistent with that of steering levels in the global ocean, which tend to be shallow in equatorial latitudes and deepen moving poleward. The overall geography of steering levels is in accordance with expectations from theory explored in previous studies (e.g., Smith and Marshall 2009; Tulloch et al. 2011). Strong suppression in the tropics is expected because it is a region of strong wave activity with $|\overline{u} - c|^2/u_{\mathrm{rms}}^2 \gg 1$.

The implied zonal average of diffusivity is shown in Fig. 9. The influence of the Kuroshio and Gulf Stream is clear at 40°N or so where relatively weak suppression and a large surface rms velocity conspire to produce a relatively strong eddy diffusivity over the upper 1000 m

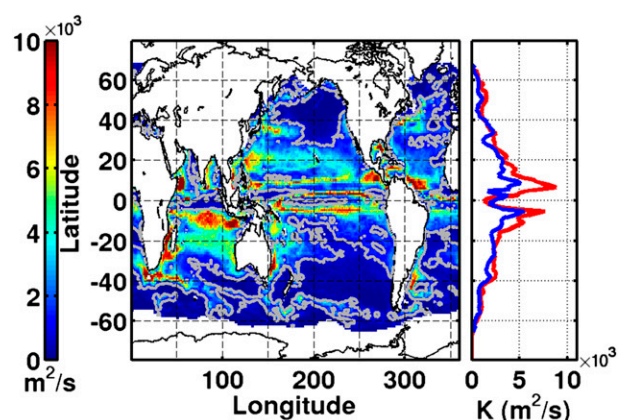FIG. 7. The eddy diffusivity ($m^2 s^{-1}$) resulting from the modulated mixing length theory, as described by Eq. (6). (left) A map, where the color is saturated at $10\,000\,m^2\,s^{-1}$, and the gray line is an isoline of $1000\,m^2\,s^{-1}$. (right) A zonal average of (left) is given in blue and the zonally averaged diffusivity of Abernathey and Marshall (2013; see also Fig. 1) is given in red.
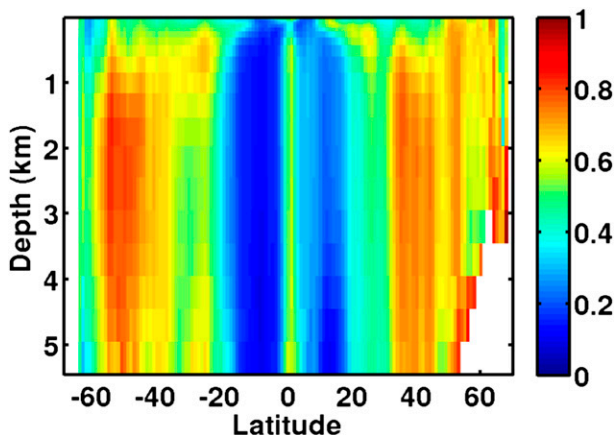
FIG. 8. The zonally averaged suppression factor $[1 + b_1|\overline{u} - c|^2/u_{rms}^2]^{-1}$ [cf. Eq. (7); nondimensional; with $b_1 = 4$]. The rms eddy velocity is taken from ECCO2 (interpolated to a 1° grid), $\overline{u}$ is taken from ECCO, and the phase speed is taken from the dataset of Hughes.
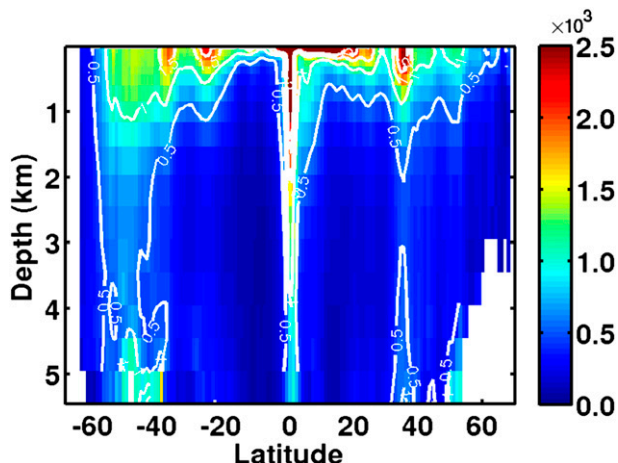
FIG. 9. The zonally averaged predicted eddy diffusivity ($m^2\,s^{-1}$), calculated using the ECCO2 u_{rms}, ECCO mean currents, an observed eddy length scale, and an observed eddy phase speed. The color is saturated at $2500\,m^2\,s^{-1}$ and white contours are shown at 0.5×10^3, 1.0×10^3, 1.5×10^3, and $2.0 \times 10^3\,m^2\,s^{-1}$.

of the ocean. In the Southern Ocean, steering levels are also at work with suppression offsetting strong surface u_{rms} but weaker suppression at depth. This leads to eddy diffusivities that have significant magnitudes even at depth.

The robust feature of Fig. 9 is that the eddy diffusivities are surface intensified over the majority of the ocean and decay rather rapidly with depth, to the extent that below 1 km they have values less than $500\,m^2\,s^{-1}$. It
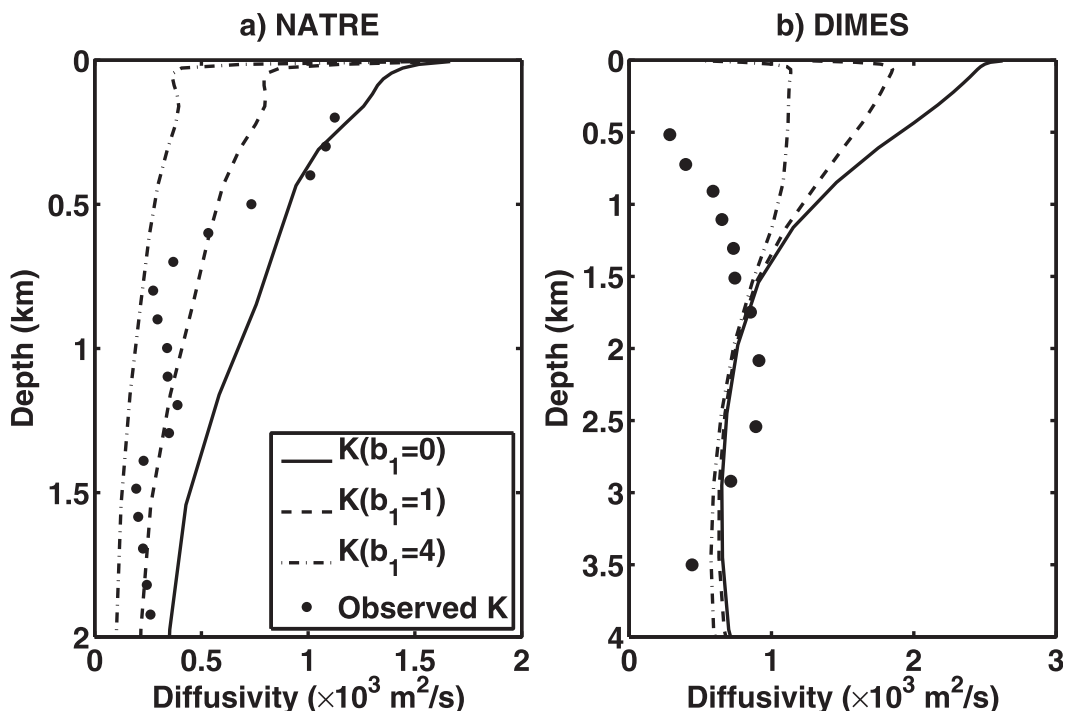
FIG. 10. Vertical profiles of diffusivity averaged over the (a) NATRE and (b) DIMES regions. Estimates from Ferrari and Polzin (2005) for NATRE and Tulloch et al. (2013, manuscript submitted to *J. Phys. Oceanogr.*) for DIMES are the solid dots, while the prediction using Eq. (6) is shown as the lines—solid for $b_1 = 0$ (no suppression), dashed for $b_1 = 1$, and dashed–dotted for $b_1 = 4$. Note the different horizontal and vertical axis scales between (a) and (b).

is difficult to make detailed comparisons with observations as there have only been two attempts to infer the vertical profile of the eddy diffusivity, namely, the North Atlantic Tracer Release Experiment (NATRE) and the Diapycnal and Isopycnal Mixing Experiment in the Southern Ocean (DIMES). Figure 10 presents our estimates of eddy diffusivity in the NATRE and DIMES regions. We present calculations with $b_1 = 0$ (no suppression), $b_1 = 1$, and $b_1 = 4$ and compare them with independent estimates reported in Ferrari and Polzin (2005) and Tulloch et al. (2013, manuscript submitted to *J. Phys. Oceanogr.*), respectively.

In the NATRE region, the diffusivity calculated using Eq. (6) matches the general shape found by Ferrari and Polzin (2005) reasonably well for all values of b_1. The magnitude is underestimated with both $b_1 = 1$ and $b_1 = 4$, while it is mostly overestimated without any suppression ($b_1 = 0$). In this instance, a value of $b_1 = 0.5$ produces the best fit. This indicates that in the NATRE region the decay of diffusivity is largely related to the decay in u_{rms} with suppression diminishing the magnitude of the diffusivity throughout the water column.

In the DIMES region the interplay between the suppression factor and the rms eddy velocity is more complicated. Unlike in NATRE, the overall shape of the diffusivity is sensitive to the choice of b_1. Indeed Tulloch et al. (2013, manuscript submitted to *J. Phys. Oceanogr.*) argue that the eddy diffusivity in DIMES may have a subsurface maximum, as plotted in Fig. 10b, which is associated with the steering level of the baroclinic waves in the ACC being at a considerable depth [see Smith and Marshall (2009)]. This offsets the decay of u_{rms} from the surface. Our application of Eq. (6) shows that increasing the influence of suppression by increasing b_1 does indeed lead to vertical structures that are more similar to the diffusivity inferred by Tulloch et al. (2013, manuscript submitted to *J. Phys. Oceanogr.*). However, we can only achieve a subsurface maximum in diffusivity for $b_1 \gg 4$ that, given the results in section 2c, would appear to be unrealistically large. However, it is clear that the application of Eq. (6) to the subsurface ocean captures the suppression of K in the upper kilometer of the DIMES region, which is the most glaring failure of the application of mixing length theory sans steering level effects.

For the development of an eddy diffusivity parameterization, it is unclear how important it is to capture the subsurface maxima apparent in the observational estimates of K because the results of Abernathey et al. (2013) indicate that the eddy stress is very sensitive to the bulk value of K in the thermocline but not as much to its vertical variations at depth. Thus, it is reasonable to anticipate that the most important feature for a parameterization to capture is suppression in the upper ocean,
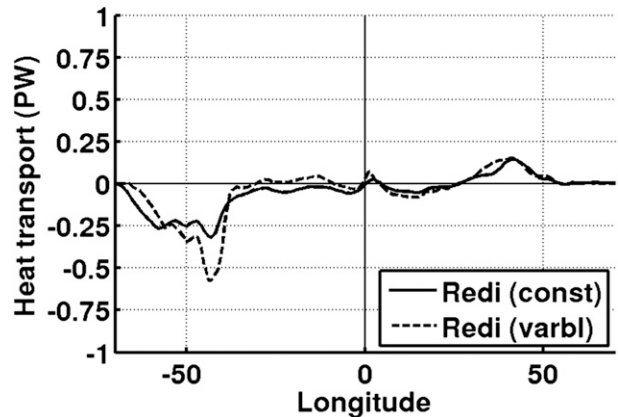

FIG. 11. The poleward heat transport (PW) from eddy mixing, using a constant diffusivity of $K = 1000 \, \mathrm{m^2 \, s^{-1}}$ and the variable diffusivity in Eq. (6).

which Fig. 10 indicates the parameterization Eq. (6) captures. Having said that, there is clearly a knowledge gap in mixing length theory for the subsurface ocean, and the discrepancies in Fig. 10 are clear motivation for further studies, observational, modeling, and theoretical, on the vertical structure of the diffusivity in the ocean.

b. Implied heat transport due to isoneutral diffusion

The diffusivity in Eq. (6) and discussed above is the cross-stream eddy diffusivity for a passive tracer [and not, e.g., buoyancy, as discussed in Smith and Marshall (2009) and Ferrari and Nikurashin (2010)]. This makes it suitable for use in eddy mixing parameterizations for passive tracers along neutral surfaces, such as that of Redi (1982).

Figure 11 compares the meridional eddy heat flux due to isoneutral mixing when a constant and a variable diffusivity is used. Large differences are evident. It should be noted, however, that the data used to obtain Fig. 11 are derived from ECCO that itself employs an isoneutral diffusion parameterization. Absent from the variable diffusivity estimate is the feedback between the parameterization and the density structure. However, our purpose here is to demonstrate that the use of a variable diffusivity might lead to rather substantial changes in parameterized fluxes. As is perhaps to be expected, the region where the greatest effect occurs is in the Southern Ocean.

4. The eddy-induced advective velocity and overturning streamfunction

The wind-driven overturning in the Southern Ocean, often referred to as the Deacon cell (e.g., Döös and Webb 1994), is largely balanced by an eddy-induced

circulation; the resulting net circulation is referred to as the residual circulation (e.g., Marshall and Radko 2003; Marshall and Speer 2012). In ocean models that do not resolve eddies, it is critically important to parameterize the eddy-induced circulation to capture the residual upwelling flux (Danabasoglu et al. 1994). Here, we therefore focus on the eddy-induced component of the circulation only.

When formulating the residual-mean momentum equations, an "eddy force" appears in the form of an eddy potential vorticity flux $\overline{\mathbf{u}'q'}$. This force results in an eddy-induced velocity (or bolus velocity) given by

$$-f\mathbf{u}* = f\partial_z\mathbf{\Psi}* \equiv \overline{\mathbf{u}'q'} \quad \text{and} \tag{9a}$$

$$w* = \mathbf{\nabla} \cdot \mathbf{\Psi}*, \tag{9b}$$

where q is the quasigeostrophic potential vorticity. As discussed in section 2, eddies tend to homogenize potential vorticity (Rhines and Young 1982; Marshall 1981; Cerovečki et al. 2009), as such a common closure is to assume that the eddies flux potential vorticity is down the large-scale gradient (Treguier et al. 1997), thus

$$\overline{\mathbf{u}'q'} \approx -K\mathbf{\nabla}\overline{q}, \tag{10}$$

where K is an eddy diffusivity. On the large scale, where the mean potential vorticity has geometrical simplicity and whose gradients do not radically change on the scale of an eddy, the diffusivity for a passive tracer and potential vorticity can be expected to be very similar (Plumb and Mahlman 1987; Cerovečki et al. 2009; Smith and Marshall 2009). We therefore assume that the diffusivity in Eq. (6), which has been the focus of our discussions thus far, can be used in Eq. (10). When mixing potential vorticity, however, care must be taken not to violate momentum constraints: the eddy potential vorticity flux may only redistribute momentum and not act as a net momentum source or sink (e.g., Welander 1973; Stewart and Thomson 1977; Thomson and Stewart 1977). There is thus a strong integral constraint on the eddy potential vorticity flux (Charney and Stern 1962; Bretherton 1966; Green 1970; Marshall 1981; Treguier et al. 1997). If the diffusivity is held constant, the integral constraint yields statements about conditions on the boundary. When the diffusivity is allowed to vary in space, as in White (1977) and Marshall (1981), the constraint can be used to yield information about the vertical structure of the eddy diffusivity.

The eddy potential vorticity flux $\overline{\mathbf{u}'q'}$ can be expressed as the sum of the eddy relative vorticity flux and the vertical divergence of eddy buoyancy fluxes (e.g., Marshall 1981; Vallis 2006), which can be related to the divergence of the Eliassen–Palm flux. This latter flux comprises Reynolds stresses (associated with lateral momentum transfer) and eddy buoyancy fluxes (e.g., Young 2012; Marshall et al. 2012). In the ocean it is thought that the buoyancy flux term dominates (e.g., Larichev and Held 1995; Treguier et al. 1997), allowing us to approximate the potential vorticity flux thus

$$\overline{\mathbf{u}'q'} \approx f\partial_z\left(\frac{\overline{\mathbf{u}'b'}}{N^2}\right). \tag{11}$$

Under the quasigeostrophic approximation, the buoyancy flux may be interpreted as the vertical divergence of an eddy form stress, which is associated with vertical transfer of horizontal momentum (Rhines and Holland 1979; Rhines and Young 1982; Greatbatch 1998) and expressing the fact that geostrophic eddies in the ocean predominantly transfer horizontal momentum vertically rather than horizontally. In this limit, the constraint reduces to

$$\int_{-H}^{0} \overline{\mathbf{u}'q'}\,dz = 0, \tag{12}$$

applied at each horizontal position in the fluid.

To enforce the constraint Eq. (12), we used a projection method inspired by the discussion in Ferrari et al. (2010). The eddy force at each level in the model is evaluated by multiplying $\mathbf{\nabla}\overline{q}$ with the eddy diffusivity. On the large scale, the relative vorticity gradient is assumed small and is ignored. However, the planetary vorticity gradient is not small and is retained (Marshall 1981; Treguier et al. 1997; Cerovečki et al. 2009). We therefore write the quasigeostrophic potential vorticity gradient as

$$\mathbf{\nabla}\overline{q} = \beta\hat{\mathbf{y}} - f\partial_z\mathbf{S}, \tag{13}$$

where $\mathbf{S} = -\mathbf{\nabla}\overline{b}/\partial_z\overline{b}$ is the mean isopycnal slope and $\hat{\mathbf{y}}$ is the meridional unit vector. The resulting vertical array of $K\mathbf{\nabla}\overline{q}$ is then expanded in terms of baroclinic modes:

$$\mathbf{\Xi}(x, y, z, t) = -\sum_{m=1}^{M} \phi_m \int_{-H}^{0} \phi_m K\mathbf{\nabla}\overline{q}\,dz, \tag{14}$$

where $\mathbf{\Xi} = [\Xi^{(x)}, \Xi^{(y)}]$, ϕ_m is the mth baroclinic mode, and M is the number of modes used (see appendix B for more details). The modal expansion has two useful properties. The first is that if the barotropic mode ($m = 0$) is set to zero, then $\mathbf{\Xi}$ satisfies the integral constraint Eq. (12). Second, a low-mode expansion of $\mathbf{\Xi}$ smooths what is an otherwise noisy field while retaining its gross vertical structure.

Following the method suggested by Treguier et al. (1997), boundary conditions at the top and the bottom
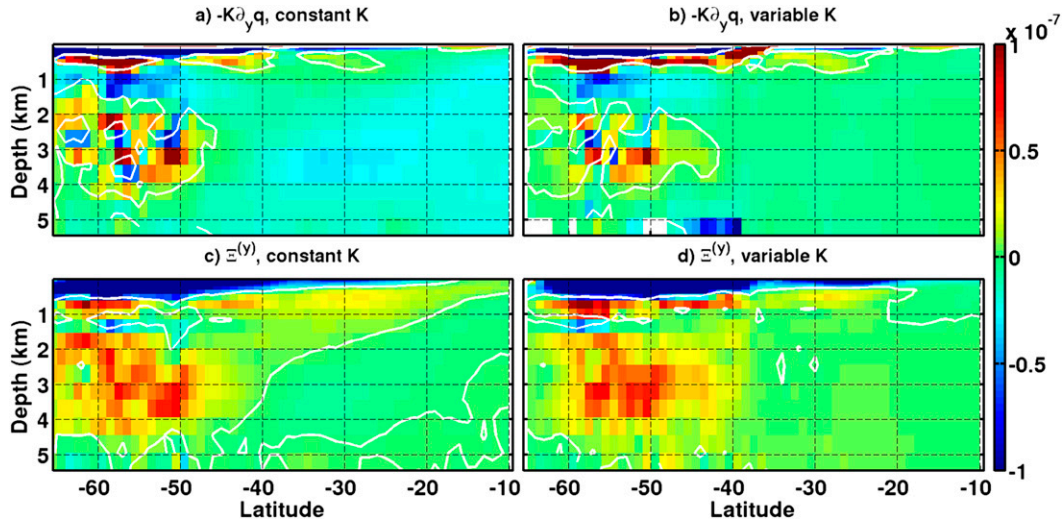
FIG. 12. Estimates of the quasigeostrophic potential vorticity eddy flux $\overline{\mathbf{u}'q'}$ (m s^{-2}). Use of the downgradient approximation Eq. (10) with (a) assuming a constant value of $K = 1000$ m^2 s^{-1} and (b) using a variable K, calculated using Eq. (6). (c),(d) The modal expansions of (a) and (b), respectively. Note that the color in all panels is saturated at $\pm 10^{-7}$ m s^{-1}.

of the water column are dealt with by using δ-function sheets of potential vorticity following the ideas of Bretherton (1966). That is, we divide the water column into three regions: the surface layer, adiabatic interior, and bottom layer. To treat the boundary, we replace the surface inhomogeneous boundary condition for buoyancy with a homogeneous one [following Bretherton (1966)]. In practice, this is achieved by setting the isopycnal slope to zero at the boundary, $\mathbf{S}|_{z=0} = 0$ and $\mathbf{S}|_{z=-H} = 0$, and taking the average quasigeostrophic potential vorticity gradient over that layer as follows:

$$
\begin{aligned}
\nabla \overline{q}_{\text{surf}} &= \frac{1}{h_{\text{surf}}} \int_{-h_{\text{surf}}}^{0} (\beta \hat{\mathbf{y}} - f \partial_z \mathbf{S}) \, dz \\
&= \beta \hat{\mathbf{y}} + \frac{f \mathbf{S}|_{z=-h_{\text{surf}}}}{h_{\text{surf}}},
\end{aligned} \tag{15a}
$$

where h_{surf} is the depth of the surface layer. Here we assume that h_{surf} is approximately the depth of the mixed layer, which we diagnose following Large et al. (1997), who defines the depth of the mixed layer to be the depth where $[b(z) - b(z = 0)]/z$ is a maximum.

An analogous expression is used to handle the bottom:

$$
\begin{aligned}
\nabla \overline{q}_{\text{bott}} &= \frac{1}{H - h_{\text{bott}}} \int_{-H}^{-h_{\text{bott}}} (\beta \hat{\mathbf{y}} - f \partial_z \mathbf{S}) \, dz \\
&= \beta \hat{\mathbf{y}} - \frac{f \mathbf{S}|_{z=-h_{\text{bott}}}}{H - h_{\text{bott}}}.
\end{aligned} \tag{15b}
$$

For simplicity, we have assumed that the thickness of this bottommost layer is the thickness of the bottom grid cell itself.

The expansion of the parameterized eddy force Ξ (which we truncate at $M = 6$) is shown in Fig. 12 using the variable K calculated from Eq. (6). It is compared to that obtained when a constant $K = 1000$ m^2 s^{-1} is assumed. The large-scale pattern of the quasigeostrophic potential vorticity gradient is consistent with previous studies (e.g., Tulloch et al. 2011). While the zonally averaged expansion in Figs. 12c and 12d does not exactly match the corresponding fields in Figs. 12a and 12b, this is to be expected. Discarding the barotropic mode enforces the integral constraint Eq. (12) by essentially removing the column mean. This manifests itself in Fig. 12 as a constant shift in value (and hence color) at each latitude when comparing Figs. 12a and 12b to Figs. 12c and 12d. Also, note how the expansion usefully acts as a low-pass filter to smooth the field and remove much of the noise.

The implied eddy-induced streamfunction for a constant and variable K are shown in Fig. 13. Both expansions are truncated at $M = 6$ (as for Fig. 12). The most striking difference between the two estimates is the position of the overturning cells. Using a variable K broadens and moves the center of the cell north compared to that obtained with a constant K.

Note how the use of a variable diffusivity has a nontrivial effect. That is, the maxima of the overturning cell in Fig. 13b now depend on local isopycnal slope and u_{rms}. The northernmost maximum in Fig. 13b is at $\sim$40°S and
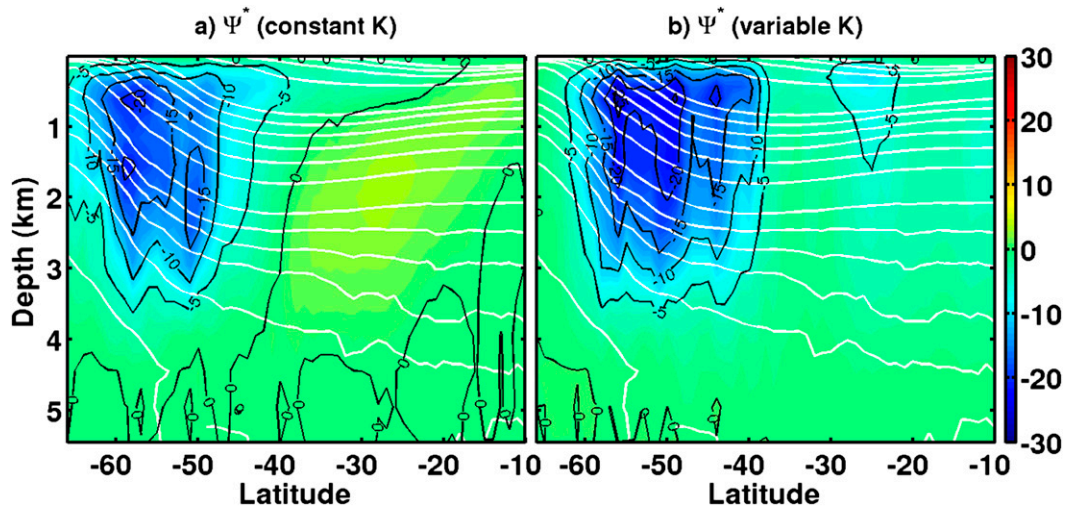
FIG. 13. The Eulerian mean overturning streamfunction [Sverdrup (Sv); $1\,\mathrm{Sv} \equiv 10^6\,\mathrm{m}^3\,\mathrm{s}^{-1}$] for the eddy-induced flow. Zonally averaged constant buoyancy surfaces are represented by the white contours. (a) A constant $K = 1000\,\mathrm{m}^2\,\mathrm{s}^{-1}$ is used, while (b) a variable K, calculated using Eq. (6), is used. Both are truncated at $M = 6$ and correspond to the quasi-potential vorticity eddy fluxes shown in Figs. 12c and 12d. Note that the color is saturated at $\pm 30\,\mathrm{Sv}$.

corresponds to the latitude of the highly energetic region downstream of the Agulhas retroflection and the Argentine Basin (see Fig. 2a). The remainder of the cell, from ~45° to ~60°S, covers the latitudinal extent of the ACC, including the regions with the steepest isopycnals. In contrast, the constant K streamfunction is centered only on the latitudes of the steepest isopycnals. The depth of the maximum value of the overturning streamfunction is also shallower than when a constant K is used. Again, this is likely the influence of the eddy kinetic energy distribution, with larger values of u_{rms} closer to the surface.

5. Discussion and conclusions

In this study, we have used mixing length theory to test an expression for the mesoscale eddy diffusivity that attempts to represent the suppression of mixing due to steering level effects. It represents a synthesis of ideas that have and are being explored in the literature and is a first step toward applying them to eddy parameterizations in global ocean climate models.

We explored a form for the eddy diffusivity given in Eq. (6), taken from Ferrari and Nikurashin (2010, see section 2). The quantities that enter in the equation are estimated from global observations of mean and eddy currents. The resulting distributions are compared to the maps of eddy diffusivity diagnosed by Abernathey and Marshall (2013) using tracer advection methods driven by satellite altimetry. We found that the suppression of the surface eddy diffusivity by steering level effects is very

significant and plays a role that is at least as important as the spatial distribution of u_{rms}. Suppression is most active where the ratio $|\bar{u} - c|^2/u_{\mathrm{rms}}^2$ is much greater than one (see Figs. 2 and 5). This occurs principally in the tropics and in high southern latitudes along the track of the ACC. This is consistent with estimates of eddy mixing rates in the Southern Ocean by Marshall et al. (2006), who find extensive regions of suppressed mixing along the track of the ACC, even though u_{rms} is at a maximum there.

Attempts to quantify the quality of the agreement between "predicted" [using Eq. (6)] and "estimated" diffusivity [from Abernathey and Marshall (2013)] enable us to explore the sensitivity of our expression to uncertain parameters that control the degree of suppression, that is, b_1 in Eq. (6). This suggests that a global value of around 4 is optimum, consistent with prior estimates of Ferrari and Nikurashin (2010) and Klocker and Abernathey (2014).

The resulting maps reveal the following:

(i) Inclusion of suppression due to steering level effects significantly improves our ability to reconstruct the spatial distributions of eddy diffusivity found by Abernathey and Marshall (2013).

(ii) Broad patterns in the diffusivity emerge that are a consequence of suppression and not merely associated with spatial distributions of u_{rms}.

(iii) Eddy diffusivities are strongly suppressed in the tropics and the ACC because $|\bar{u} - c|^2/u_{\mathrm{rms}}^2 \gg 1$ in these regions, reducing the unrealistically large values of mixing evident in unsuppressed maps.

We applied the theory developed for the ocean surface to the subsurface ocean. Evaluating the efficacy of applying the theory to the entire water column is made difficult by the paucity of subsurface measurements of mixing. Our results display some features that would be expected from previous works on steering level effects on mixing such as strong suppression in mixing in the upper kilometer along the path of the ACC (Smith and Marshall 2009; Abernathey et al. 2010; Ferrari and Nikurashin 2010); however, other aspects, such as anticipated subsurface maxima, indicate that the theory for subsurface mixing is incomplete and requires additional development. To help bridge this knowledge gap in our understanding of how the vertical structure of K is set, numerical studies and observational campaigns like DIMES will be invaluable in making further progress.

Finally, we developed a methodology, inspired by the work of Ferrari et al. (2010), to obtain the eddy-induced advective velocity implied by potential vorticity mixing (as opposed to buoyancy mixing), in which a vertical projection onto orthogonal baroclinic modes is carried out. The approach guarantees that eddies only redistribute momentum in the vertical. The resulting eddy-induced overturning streamfunction shows that steering level effects, as encapsulated in our spatially varying diffusivity, play an important role in setting the amplitude and pattern of eddy-induced overturning in the Southern Ocean.

We note in conclusion that the approach outlined here lends itself to a parameterization of mesoscales that can be used in primitive equation ocean models as they integrate forward in time. In a future study, we will bring the ideas explored here in to a full parametric representation of mesoscales and evaluate it as a global ocean model.

APPENDIX A

A Discussion on the Cross-Stream Diffusivity

Ferrari and Nikurashin (2010) write the cross-stream eddy diffusivity for a purely zonal flow at the surface of the ocean as [see their Eq. (14)]

$$K_\perp^{\mathrm{FN}} = \frac{K_0^{\mathrm{FN}}}{1 + \gamma^{-2}k^2(\overline{u} - c)^2} \quad \text{and} \quad \text{(A1a)}$$

$$K_0^{\mathrm{FN}} = \frac{k^2}{|\mathbf{k}|^2}\gamma^{-1}u_{\mathrm{rms}}^2, \quad \text{(A1b)}$$

where γ is the inverse of the decorrelation time scale of the waves/eddies stirring the tracer, $|\mathbf{k}| = \sqrt{k^2 + l^2}$ is the eddy wavenumber, $\overline{u}$ is the mean zonal flow, and c is the zonal phase speed of the waves/eddies. Note that Eq. (A1) is identical to Eq. (5). As in Ferrari and Nikurashin (2010), we assume that the energy-containing eddies are isotropic $|\mathbf{k}|^2 = 2k^2$, allowing us to write

$$K_0^{\mathrm{FN}} = \frac{1}{2}\gamma^{-1}u_{\mathrm{rms}}^2. \quad \text{(A2)}$$

We also assume that the eddy decorrelation time scale is proportional to the eddy strain rate in a turbulent field (Salmon 1998):

$$\gamma^2 \propto |\mathbf{k}|^2 u_{\mathrm{rms}}^2. \quad \text{(A3)}$$

We can therefore write K_0^{FN} as

$$K_0 = \frac{1}{2}b_0|\mathbf{k}|^{-1}u_{\mathrm{rms}}, \quad \text{(A4)}$$

where b_0 is a constant of proportionality.

As was done in Ferrari and Nikurashin (2010), we simplify the denominator of $K_\perp^{\mathrm{FN}}$ in Eq. (A1a) by exploiting the proportionality between the eddy decorrelation time scale and the eddy strain rate. We write

$$K_\perp = \frac{\frac{1}{2}b_0|\mathbf{k}|^{-1}u_{\mathrm{rms}}}{1 + b_1(\overline{u} - c)^2/u_{\mathrm{rms}}^2}. \quad \text{(A5)}$$

In a purely monochromatic eddy field $b_1 = b_0^2/2$, but in general the ocean eddy field is multichromatic and then $b_1 \neq b_0^2/2$, as explained in Holloway and Kristmannsson (1984) and Ferrari and Nikurashin (2010).

The constants b_0 and b_1 need to be determined empirically. Ferrari and Nikurashin (2010) estimated them by fitting Eq. (A5) to surface estimates of $K_\perp$ based on altimetric data from the ACC and the approach of Nakamura (1996). They assumed that the eddy phase speed is proportional to the mean ACC velocity $c = (1 - \alpha)\overline{u}$, and from that $2\alpha^2 b_1 \approx 4$. In the ACC $\alpha \approx 0.8$ (using Hughes phase speed map and ECCO surface zonal velocities), giving $b_1 \approx 4$. However, the value of b_1 inferred by this method is quite sensitive to the value of α. They also recast the numerator of Eq. (A5) in terms of sea

surface height fluctuations, so it is not quite possible to infer b_0 from their work.

The recent work of Klocker and Abernathey (2014) gives a more direct estimate of b_0 and b_1 at the surface. They use satellite-derived eddy surface velocities for a sector in the eastern Pacific and systematically vary the mean zonal flow to estimate K_0, which occurs at the zonal velocity where the diffusivity is a maximum (i.e., when $\overline{u} = c$). They show that

$$K_0^{\text{KA}} = \Gamma L_{\text{eddy}} u_{\text{rms}} \qquad (A6a)$$

provides a very good fit for their inferred (maximum) unsuppressed diffusivity, where L_{eddy} is the eddy diameter as measured by Chelton et al. (2011). Here, Γ is a mixing efficiency. They then fit the diffusivity inferred from tracers stirred by satellite velocities and find that[A1]

$$K_\perp^{\text{KA}} = \frac{K_0^{\text{KA}}}{1 + 4\Gamma^2\pi^2(\overline{u} - c)^2/u_{\text{rms}}^2} \qquad (A6b)$$

is a very good estimator of the eddy diffusivity poleward of $\pm 18°$ of latitude. By comparing Eq. (A5) with Eq. (A6) and using the relation $|\mathbf{k}| = 2\pi/L_{\text{eddy}}$, we find that $b_0 = 4\Gamma\pi$ and $b_1 = 4\Gamma^2\pi^2$. Klocker and Abernathey (2014) show that $\Gamma = 0.35$ is a reasonable estimate of the mixing efficiency; using this value yields $b_0 \approx 2.2$ and $b_1 \approx 4.4$. However, the value of b_1 is fairly sensitive to Γ; for instance, if $\Gamma = 1/2$, we obtain $b_1 = \pi^2 \approx 10$. The sensitivity of the predicted diffusivity to the value of b_1 is discussed in detail in sections 2c and 3 and shown in Fig. 7.

Substituting b_0 into Eq. (A5) gives the form of the diffusivity in Eq. (6) for the surface:

$$K = u_{\text{rms}} \frac{\Gamma L_{\text{eddy}}}{1 + b_1|\overline{u} - c|^2/u_{\text{rms}}^2}. \qquad (A7)$$

There are a number of assumptions made in the derivation of Eq. (A7) that require some discussion. First, eddies are assumed to propagate at some characteristic phase speed. Observations confirm that sea surface height anomalies propagate at the same speed regardless of size (Wunsch 2011). Second, the studies of Ferrari and Nikurashin (2010) and Naveira Garabato et al.

(2011) focused on approximately zonally uniform flows. Eddies and mean currents tend to follow contours of constant potential vorticity rather than lines of constant latitude, thus it would be more accurate to take the difference between the velocity of the mean flow $\overline{\mathbf{u}}$ and the eddy phase speed in the direction of the mean flow $c \cdot (\overline{\mathbf{u}}/|\overline{\mathbf{u}}|)$. We have verified that only considering the zonal component is a good approximation at large scales, such as those considered by this study. For finer scales, it is likely that the meridional component is nontrivial.

As stated above, if the eddy field were purely monochromatic, the two constants should be related as $b_1 = b_0^2/2$. The fact that this relation is only out by a factor of $\sqrt{2} \approx 1.4$ is an indication that the eddy field poleward of $\pm 18°$ is quite close to being monochromatic or at least that the tracer stirring is dominated by eddies with scale L_{eddy}.

Ferrari and Nikurashin (2010) and Klocker and Abernathey (2014) only consider the eddy diffusivity at the surface. To extend Eq. (A7) to depth we need to compute the ratio $|\mathbf{k}|^2|\overline{u} - c|^2/\gamma^2$, that is, the squared ratio of the eddy decorrelation time scale to the eddy propagation time scale (with respect to the mean flow). Here we assume that the eddy decorrelation time scale is independent of depth because eddies tend to have equivalent barotropic structures with a self-similar evolution at all depths, leading to Eq. (6), restated here for completeness:

$$K = u_{\text{rms}} \frac{\Gamma L_{\text{eddy}}}{1 + b_1|\overline{u} - c|^2/u_{\text{rms}}^2(z = 0)}.$$

While assuming γ is constant with depth is sensible, it must be regarded as an ansatz to be verified with numerical simulations of geostrophic turbulent fields. We use the surface value to infer γ, which is a convenient but arbitrary choice. If the structure is equivalent barotropic, this arbitrariness is absorbed in the coefficient b_1.

APPENDIX B

Expansion of the Eddy Flux of Quasigeostrophic Potential Vorticity

To expand the quasigeostrophic potential vorticity flux in terms of baroclinic modes, we begin by defining

$$\mathbf{\Xi}(x, y, z, t) = \overline{\mathbf{u}'q'}, \qquad (B1)$$

where $\mathbf{\Xi} = (\Xi^{(x)}, \Xi^{(y)})$. We can expand Eq. (B1) using the baroclinic modes as an orthonormal basis:

[A1] The form that Klocker and Abernathey (2014) uses is $K_\perp^{\text{KA}} = K_0^{\text{KA}}[1 + |\mathbf{k}|^2\gamma^{-2}(\overline{u} - c)^2]^{-1}$. However, they set $|\mathbf{k}| = 2\pi/L_{\text{eddy}}$ and $\gamma^{-1} = \Gamma L_{\text{eddy}} u_{\text{rms}}^{-1}$ to obtain their fit for $K_\perp^{\text{KA}}$, which leads us to the form in Eq. (A6b).

$$\Xi(x,y,z,t) = \sum_{m=0}^{\infty} \phi_m \Xi_m(x,y,t), \qquad \text{(B2)}$$

where ϕ_m is the mth eigenvector from the Rossby equation for a resting ocean, which is obtained by solving the Sturm–Liouville equation (e.g., Smith 2007),

$$\left(k_m^2 + \frac{d}{dz} \frac{f^2}{N^2} \frac{d}{dz} \right) \phi_m = 0, \qquad \text{(B3a)}$$

which has boundary conditions

$$\left. \frac{d\phi_m}{dz} \right|_{z=0} = \left. \frac{d\phi_m}{dz} \right|_{z=-H} = 0. \qquad \text{(B3b)}$$

Here, k_m^2 is the eigenvalue of the problem and is the Rossby deformation wavenumber (the inverse of the Rossby radius of deformation). The orthogonality condition is given by

$$\int_{-H}^0 \phi_m \phi_n \, dz = \delta_{mn}, \qquad \text{(B4)}$$

where

$$\delta_{nm} = \begin{cases} 1 & \text{if} \quad n = m \\ 0 & \text{if} \quad n \neq m \end{cases} \qquad \text{(B5)}$$

is the Kronecker delta. An important property of the solution for $m > 0$ is that the vertical integral of each mode is zero:

$$\int_{-H}^0 \phi_m \, dz = 0, \qquad \text{(B6)}$$

thus an expansion in terms of these baroclinic modes will automatically satisfy this integral constraint, vis-à-vis Eq. (12). We therefore discard the $m = 0$ term (the barotropic mode) because the vertical integral of ϕ_0 is nonzero.

To find the expansion coefficients (e.g., Jackson 1998, chapter 2.8) for the modal expansion in Eq. (14) we can write the function for the eddy-induced quasigeostrophic potential vorticity flux Ξ, defined in Eq. (B1), in terms of an expansion of eigenfunctions ϕ from solving Eq. (B3a) as

$$\Xi(x,y,z,t) = \sum_{m=1}^{\infty} \phi_m(z) \Xi_m(x,y,t), \qquad \text{(B7)}$$

which we can then manipulate, using the orthogonality condition Eq. (B4), to find the expansion coefficients Ξ_m

$$\int_{-H}^0 \Xi(x,y,z,t) \phi_n(z) \, dz$$

$$= \int_{-H}^0 \sum_{m=1}^{\infty} \phi_m(z) \Xi_m(x,y,t) \phi_n(z) \, dz, \qquad \text{(B8a)}$$

$$= \sum_{m=1}^{\infty} \Xi_m(x,y,t) \int_{-H}^0 \phi_m(z) \phi_n(z) \, dz, \qquad \text{(B8b)}$$

$$= \sum_{m=1}^{\infty} \Xi_m(x,y,t) \delta_{mn}, \qquad \text{(B8c)}$$

where δ_{mn} is the Kronecker delta [see Eq. (B5)]. This allows us to write the expansion coefficient as

$$\Xi_n(x,y,t) = \int_{-H}^0 \Xi(x,y,z,t) \phi_n(z) \, dz. \qquad \text{(B9)}$$

Using the closure in Eq. (10), and the definition of Ξ in Eq. (B1), we obtain the expansion

$$\Xi(x,y,z,t) = -\sum_{m=1}^{M} \phi_m \int_{-H}^0 \phi_m K \nabla \overline{q} \, dz, \qquad \text{(B10)}$$

where we have truncated at the Mth mode.

REFERENCES

Abernathey, R., and J. C. Marshall, 2013: Global surface eddy diffusivities derived from satellite altimetry. *J. Geophys. Res. Oceans,* **118,** 901–916, doi:10.1002/jgrc.20066.

——, ——, M. Mazloff, and E. Shuckburgh, 2010: Enhancement of mesoscale eddy stirring at steering levels in the Southern Ocean. *J. Phys. Oceanogr.,* **40,** 170–184, doi:10.1175/2009JPO4201.1.

——, D. Ferreira, and A. Klocker, 2013: Diagnostics of isopycnal mixing in a circumpolar channel. *Ocean Modell.,* **72,** 1–16, doi:10.1016/j.ocemod.2013.07.004.

Bower, A. S., 1991: A simple kinematic mechanism for mixing fluid parcels across a meandering jet. *J. Phys. Oceanogr.,* **21,** 173–180, doi:10.1175/1520-0485(1991)021<0173:ASKMFM>2.0.CO;2.

——, and M. S. Lozier, 1994: A closer look at particle exchange in the Gulf Stream. *J. Phys. Oceanogr.,* **24,** 1399–1418, doi:10.1175/1520-0485(1994)024<1399:ACLAPE>2.0.CO;2.

Bretherton, F. P., 1966: Critical layer instability in baroclinic flows. *Quart. J. Roy. Meteor. Soc.,* **92,** 325–334, doi:10.1002/qj.49709239302.

Cerovečki, I., R. A. Plumb, and W. Heres, 2009: Eddy transport and mixing in a wind- and buoyancy-driven jet on the sphere. *J. Phys. Oceanogr.,* **39,** 1133–1149, doi:10.1175/2008JPO3596.1.

Charney, J. G., and M. E. Stern, 1962: On the stability of internal baroclinic jets in a rotating atmosphere. *J. Atmos. Sci.,* **19,** 159–172, doi:10.1175/1520-0469(1962)019<0159:OTSOIB>2.0.CO;2.

Chelton, D. B., M. G. Schlax, and R. M. Samelson, 2011: Global observations of nonlinear mesoscale eddies. *Prog. Oceanogr.,* **91,** 167–216, doi:10.1016/j.pocean.2011.01.002.

Danabasoglu, G., and J. C. Marshall, 2007: Effects of vertical variations of thickness diffusivity in an ocean general circulation model. *Ocean Modell.,* **18,** 122–141, doi:10.1016/j.ocemod.2007.03.006.

——, J. C. McWilliams, and P. R. Gent, 1994: The role of mesoscale tracer transports in the global ocean circulation. *Science,* **264,** 1123–1126, doi:10.1126/science.264.5162.1123.

Davis, R. E., 1991: Observing the general circulation with floats. *Deep-Sea Res.,* **38A** (Suppl. 1), S531–S571, doi:10.1016/S0198-0149(12)80023-9.

Döös, K., and D. J. Webb, 1994: The Deacon cell and the other meridional cells of the Southern Ocean. *J. Phys. Oceanogr.,* **24,** 429–442, doi:10.1175/1520-0485(1994)024<0429:TDCATO>2.0.CO;2.

Eden, C., and R. J. Greatbatch, 2008: Diapycnal mixing by meso-scale eddies. *Ocean Modell.,* **23,** 113–120, doi:10.1016/j.ocemod.2008.04.006.

Ferrari, R., and K. L. Polzin, 2005: Finescale structure of the *T–S* relation in the eastern North Atlantic. *J. Phys. Oceanogr.,* **35,** 1437–1454, doi:10.1175/JPO2763.1.

——, and M. Nikurashin, 2010: Suppression of eddy diffusivity across jets in the Southern Ocean. *J. Phys. Oceanogr.,* **40,** 1501–1519, doi:10.1175/2010JPO4278.1.

——, S. M. Griffies, A. J. G. Nurser, and G. K. Vallis, 2010: A boundary-value problem for the parameterized mesoscale eddy transport. *Ocean Modell.,* **32,** 143–156, doi:10.1016/j.ocemod.2010.01.004.

Ferreira, D., J. C. Marshall, and P. Heimbach, 2005: Estimating eddy stresses by fitting dynamics to observations using a residual-mean ocean circulation model and its adjoint. *J. Phys. Oceanogr.,* **35,** 1891–1910, doi:10.1175/JPO2785.1.

Gent, P. R., and J. C. McWilliams, 1990: Isopycnal mixing in ocean circulation models. *J. Phys. Oceanogr.,* **20,** 150–155, doi:10.1175/1520-0485(1990)020<0150:IMIOCM>2.0.CO;2.

Greatbatch, R. J., 1998: Exploring the relationship between eddy-induced transport velocity, vertical momentum transfer, and the isopycnal flux of potential vorticity. *J. Phys. Oceanogr.,* **28,** 422–432, doi:10.1175/1520-0485(1998)028<0422:ETRBEI>2.0.CO;2.

Green, J. S. A., 1970: Transfer properties of the large-scale eddies and the general circulation of the atmosphere. *Quart. J. Roy. Meteor. Soc.,* **96,** 157–185, doi:10.1002/qj.49709640802.

Griffies, S. M., and Coauthors, 2009: Coordinated Ocean–Ice Reference Experiments (COREs). *Ocean Modell.,* **26,** 1–46, doi:10.1016/j.ocemod.2008.08.007.

Haine, T. W. N., and J. C. Marshall, 1998: Gravitational, symmetric, and baroclinic instability of the ocean mixed layer. *J. Phys. Oceanogr.,* **28,** 634–658, doi:10.1175/1520-0485(1998)028<0634:GSABIO>2.0.CO;2.

Holloway, G., 1986: Estimation of oceanic eddy transports from satellite altimetry. *Nature,* **323,** 243–244, doi:10.1038/323243a0.

——, and S. S. Kristmannsson, 1984: Stirring and transport of tracer fields by geostrophic turbulence. *J. Fluid Mech.,* **141,** 27–50, doi:10.1017/S0022112084000720.

Hughes, C. W., 2005: Nonlinear vorticity balance of the Antarctic Circumpolar Current. *J. Geophys. Res.,* **110,** C11008, doi:10.1029/2004JC002753.

——, M. S. Jones, and S. Carnochan, 1998: Use of transient features to identify eastward currents in the Southern Ocean. *J. Geophys. Res.,* **103,** 2929, doi:10.1029/97JC02442.

Jackson, J. D., 1998: *Classical Electrodynamics*. 3rd ed. Wiley, 808 pp.

Killworth, P. D., 1997: On the parameterization of eddy transfer. Part I. Theory. *J. Mar. Res.,* **55,** 1171–1197, doi:10.1357/0022240973224102.

Klocker, A., and R. P. Abernathey, 2014: Global patterns of mesoscale eddy properties and diffusivities. *J. Phys. Oceanogr.,* **44,** 1030–1046, doi:10.1175/JPO-D-13-0159.1.

——, R. Ferrari, and J. H. LaCasce, 2012a: Estimating suppression of eddy mixing by mean flows. *J. Phys. Oceanogr.,* **42,** 1566–1576, doi:10.1175/JPO-D-11-0205.1.

——, ——, ——, and S. Merrifield, 2012b: Reconciling float-based and tracer-based estimates of eddy diffusivities. *J. Mar. Res.,* **70,** 569–602, doi:10.1357/002224012805262743.

Lagerloef, G. S. E., G. T. Mitchum, R. B. Lukas, and P. P. Niiler, 1999: Tropical Pacific near-surface currents estimated from altimeter, wind, and drifter data. *J. Geophys. Res.,* **104,** 23 313–23 326, doi:10.1029/1999JC900197.

Large, W. G., G. Danabasoglu, S. C. Doney, and J. C. McWilliams, 1997: Sensitivity to surface forcing and boundary layer mixing in a global ocean model: Annual-mean climatology. *J. Phys. Oceanogr.,* **27,** 2418–2447, doi:10.1175/1520-0485(1997)027<2418:STSFAB>2.0.CO;2.

Larichev, V. D., and I. M. Held, 1995: Eddy amplitudes and fluxes in a homogeneous model of fully developed baroclinic instability. *J. Phys. Oceanogr.,* **25,** 2285–2297, doi:10.1175/1520-0485(1995)025<2285:EAAFIA>2.0.CO;2.

Ledwell, J. R., A. J. Watson, and C. S. Law, 1998: Mixing of a tracer in the pycnocline. *J. Geophys. Res.,* **103,** 21 499–21 529, doi:10.1029/98JC01738.

Lozier, M. S., and D. Bercovici, 1992: Particle exchange in an unstable jet. *J. Phys. Oceanogr.,* **22,** 1506–1516, doi:10.1175/1520-0485(1992)022<1506:PEIAUJ>2.0.CO;2.

Marshall, D. P., J. R. Maddison, and P. S. Berloff, 2012: A framework for parameterizing eddy potential vorticity fluxes. *J. Phys. Oceanogr.,* **42,** 539–557, doi:10.1175/JPO-D-11-048.1.

Marshall, J. C., 1981: On the parameterization of geostrophic eddies in the ocean. *J. Phys. Oceanogr.,* **11,** 257–271, doi:10.1175/1520-0485(1981)011<0257:OTPOGE>2.0.CO;2.

——, and T. Radko, 2003: Residual-mean solutions for the Antarctic Circumpolar Current and its associated overturning circulation. *J. Phys. Oceanogr.,* **33,** 2341–2354, doi:10.1175/1520-0485(2003)033<2341:RSFTAC>2.0.CO;2.

——, and K. Speer, 2012: Closure of the meridional overturning circulation through Southern Ocean upwelling. *Nat. Geosci.,* **5,** 171–180, doi:10.1038/ngeo1391.

——, E. Shuckburgh, H. Jones, and C. Hill, 2006: Estimates and implications of surface eddy diffusivity in the Southern Ocean derived from tracer transport. *J. Phys. Oceanogr.,* **36,** 1806–1821, doi:10.1175/JPO2949.1.

Menemenlis, D., J.-M. Campin, P. Heimbach, C. Hill, T. Lee, A. Nguyen, M. Schodlok, and H. Zhang, 2008: ECCO2: High resolution global ocean and sea ice data synthesis. *Mercator Ocean Quarterly Newsletter,* No. 31, Mercator Ocean, Ramonville Saint-Agne, France, 13–21.

Nakamura, N., 1996: Two-dimensional mixing, edge formation, and permeability diagnosed in an area coordinate. *J. Atmos. Sci.,* **53,** 1524–1537, doi:10.1175/1520-0469(1996)053<1524:TDMEFA>2.0.CO;2.

Naveira Garabato, A. C., R. Ferrari, and K. L. Polzin, 2011: Eddy stirring in the Southern Ocean. *J. Geophys. Res.,* **116,** C09019, doi:10.1029/2010JC006818.

Osborn, T. R., and C. S. Cox, 1972: Oceanic fine structure. *Geophys. Fluid Dyn.,* **3,** 321–345, doi:10.1080/03091927208236085.

Plumb, R. A., and J. D. Mahlman, 1987: The zonally averaged transport characteristics of the GFDL general circulation/transport model. *J. Atmos. Sci.,* **44,** 298–327, doi:10.1175/1520-0469(1987)044<0298:TZATCO>2.0.CO;2.

Poulain, P.-M., and P. P. Niiler, 1989: Statistical analysis of the surface circulation in the California Current system using

satellite-tracked drifters. *J. Phys. Oceanogr.,* **19,** 1588–1603, doi:10.1175/1520-0485(1989)019<1588:SAOTSC>2.0.CO;2.

Prandtl, L., 1925: Bericht über Untersuchungen zur ausgebildeten Turbulenz. *Z. Angew. Math. Mech.,* **5,** 136–139.

Redi, M. H., 1982: Oceanic isopycnal mixing by coordinate rotation. *J. Phys. Oceanogr.,* **12,** 1154–1158, doi:10.1175/1520-0485(1982)012<1154:OIMBCR>2.0.CO;2.

Rhines, P. B., and W. R. Holland, 1979: A theoretical discussion of eddy-driven mean flows. *Dyn. Atmos. Oceans,* **3,** 289–325, doi:10.1016/0377-0265(79)90015-0.

——, and W. R. Young, 1982: Homogenization of potential vorticity in planetary gyres. *J. Fluid Mech.,* **122,** 347–367, doi:10.1017/S0022112082002250.

Sallée, J. B., K. Speer, R. Morrow, and R. Lumpkin, 2008: An estimate of Lagrangian eddy statistics and diffusion in the mixed layer of the Southern Ocean. *J. Mar. Res.,* **66,** 441–463, doi:10.1357/002224008787157458.

——, ——, and S. R. Rintoul, 2011: Mean-flow and topographic control on surface eddy-mixing in the Southern Ocean. *J. Mar. Res.,* **69,** 753–777, doi:10.1357/002224011799849408.

Salmon, R., 1998: *Lectures on Geophysical Fluid Dynamics.* Oxford University Press, 378 pp.

Smith, K. S., 2007: The geography of linear baroclinic instability in Earth's oceans. *J. Mar. Res.,* **65,** 655–683, doi:10.1357/002224007783649484.

——, and J. C. Marshall, 2009: Evidence for enhanced eddy mixing at middepth in the Southern Ocean. *J. Phys. Oceanogr.,* **39,** 50–69, doi:10.1175/2008JPO3880.1.

Stewart, R., and R. E. Thomson, 1977: Re-examination of vorticity transfer theory. *Proc. Roy. Soc.,* **354,** 1–8, doi:10.1098/rspa.1977.0053.

Stone, P. H., 1972: A simplified radiative-dynamical model for the static stability of rotating atmospheres. *J. Atmos. Sci.,* **29,** 405–418, doi:10.1175/1520-0469(1972)029<0405:ASRDMF>2.0.CO;2.

Swenson, M. S., and P. P. Niiler, 1996: Statistical analysis of the surface circulation of the California Current. *J. Geophys. Res.,* **101,** 22 631–22 645, doi:10.1029/96JC02008.

Taylor, G. I., 1922: Diffusion by continuous movements. *Proc. London Math. Soc.,* **s2-20,** 196–212, doi:10.1112/plms/s2-20.1.196.

Thompson, A. F., and W. R. Young, 2006: Scaling baroclinic eddy fluxes: Vortices and energy balance. *J. Phys. Oceanogr.,* **36,** 720–738, doi:10.1175/JPO2874.1.

Thomson, R. E., and R. Stewart, 1977: The balance and redistribution of potential vorticity within the ocean. *Dyn. Atmos. Oceans,* **1,** 299–321, doi:10.1016/0377-0265(77)90019-7.

Treguier, A.-M., I. M. Held, and V. D. Larichev, 1997: Parameterization of quasigeostrophic eddies in primitive equation ocean models. *J. Phys. Oceanogr.,* **27,** 567–580, doi:10.1175/1520-0485(1997)027<0567:POQEIP>2.0.CO;2.

Tulloch, R., J. C. Marshall, and K. S. Smith, 2009: Interpretation of the propagation of surface altimetric observations in terms of planetary waves and geostrophic turbulence. *J. Geophys. Res.,* **114,** C02005, doi:10.1029/2008JC005055.

——, ——, C. Hill, and K. S. Smith, 2011: Scales, growth rates, and spectral fluxes of baroclinic instability in the ocean. *J. Phys. Oceanogr.,* **41,** 1057–1076, doi:10.1175/2011JPO4404.1.

Vallis, G. K., 2006: *Atmospheric and Oceanic Fluid Dynamics: Fundamentals and Large-Scale Circulation.* Cambridge University Press, 745 pp.

Visbeck, M., J. C. Marshall, T. W. N. Haine, and M. Spall, 1997: Specification of eddy transfer coefficients in coarse-resolution ocean circulation models. *J. Phys. Oceanogr.,* **27,** 381–402, doi:10.1175/1520-0485(1997)027<0381:SOETCI>2.0.CO;2.

Welander, P., 1973: Lateral friction in the oceans as an effect of potential vorticity mixing. *Geophys. Fluid Dyn.,* **5,** 173–189, doi:10.1080/03091927308236114.

White, A. A., 1977: The surface flow in a statistical climate model—A test of a parameterization of large-scale momentum fluxes. *Quart. J. Roy. Meteor. Soc.,* **103,** 93–119, doi:10.1002/qj.49710343506.

Wunsch, C., 2011: The decadal mean ocean circulation and Sverdrup balance. *J. Mar. Res.,* **69,** 417–434, doi:10.1357/002224011798765303.

——, P. Heimbach, R. M. Ponte, I. Fukumori, and ECCO-GODAE Consortium Members, 2009: The global general circulation of the ocean estimated by the ECCO-Consortium. *Oceanography,* **22,** 88–103, doi:10.5670/oceanog.2009.41.

Young, W. R., 2012: An exact thickness-weighted average formulation of the Boussinesq equations. *J. Phys. Oceanogr.,* **42,** 692–707, doi:10.1175/JPO-D-11-0102.1.

Zhurbas, V., and I. S. Oh, 2004: Drifter-derived maps of lateral diffusivity in the Pacific and Atlantic Oceans in relation to surface circulation patterns. *J. Geophys. Res.,* **109,** C05015, doi:10.1029/2003JC002241.